J. Math. Biology (1982) 13: 345–369

Journal of
Mathematical
Biology

The Nature of the Coupling Between Segmental Oscillators of the Lamprey Spinal Generator for Locomotion: A Mathematical Model

Avis H. Cohen[1], Philip J. Holmes[2] and Richard H. Rand[2]

[1] Department of Physiology, School of Veterinary Medicine and
[2] Department of Theoretical and Applied Mechanics and Center for Applied Mathematics, Cornell University, Ithaca, NY 14853, USA

Abstract. We present a theoretical model which is used to explain the intersegmental coordination of the neural networks responsible for generating locomotion in the isolated spinal cord of lamprey.

A simplified mathematical model of a limit cycle oscillator is presented which consists of only a single dependent variable, the phase $\theta(t)$. By coupling N such oscillators together we are able to generate stable phase locked motions which correspond to traveling waves in the spinal cord, thus simulating "fictive swimming". We are also able to generate irregular "drifting" motions which are compared to the experimental data obtained from cords with selective surgical lesions.

Key words: Locomotion – Pattern generator – Dynamical systems – Oscillators

1. Introduction and Summary of Experimental Results

For 20 years it has been known that there are neural networks which can generate temporally patterned sequences of signals. By definition a pattern generating network requires neither sensory feedback nor phasic (time-varying) descending control, although afferent (input) signals may strongly influence the output of the network. The existence of pattern generators was first documented in a relatively simple invertebrate nervous system (Wilson, 1961). It is now clear the mammalian nervous systems also contain neuronal ensembles which can generate quite complex motor patterns (e.g. locomotion, scratching) in the absence of any phasic sensory information or supraspinal control (Grillner and Zangger, 1975; Vidal et al., 1979; Grillner, 1975; Berkenblitt et al., 1978).

Some progress has been made in understanding the cellular organization of pattern generating networks found in invertebrates (Selverston et al., 1976; Poon et al., 1978; Getting et al., 1980). Models have been proposed to explain how the networks, as presently understood, could generate their respective patterns (Friesen and Stent, 1977; Kristan, 1977). Although the models have all had some limitations

0303–6812/82/0013/0345/$05.00

and have upon occasion needed major revisions (cf. Selverston, 1980), they have offered a useful framework for discussion of further research. Models have played a much smaller role in studies of vertebrates' central pattern generators (CPG's) since so little is known of their underlying cellular structure (see however, Berkenblitt et al., 1978).

In general, the pattern generating networks that are being studied produce cyclic patterns of muscle activity. In several systems the activity of two muscle groups simply alternate in time. Even with more complex motor patterns like mammalian locomotion, functional groups of muscles alternate with only a few muscles deviating from this simple pattern. The neuronal pattern generators controlling these movements are often conceptualized as oscillators, or groups of coupled oscillators. However, little use has been made of oscillator theory to understand them (see however, Pavlidis and Pinsker, 1977; Glass and Young, 1979).

The lamprey is a primitive vertebrate which has been utilized to facilitate the study of the vertebrate CPG for locomotion. The spinal cord of the lamprey has several advantages over those of more highly evolved vertebrates. First, the cord is thin, transparent and contains relatively few cells while retaining the basic vertebrate organization (cf. Rovainen, 1979). Second, the spinal cord can be removed from the animal, placed in a bath containing physiological saline and kept for up to a week without apparent deterioration (Rovainen, 1979). Under such *in vitro* conditions the chemical environment can easily be altered while monitoring the activity in the ventral roots which carry the motor output of the cord (Fig. 1.1). Using this procedure it has been shown that adding various neuro-pharmacological agents to the bath can induce bursts of ventral root (VR) activity with the same temporal pattern as the activity of the myotomal or body muscles of intact swimming fish (Cohen and Wallén, 1980; Poon, 1980).

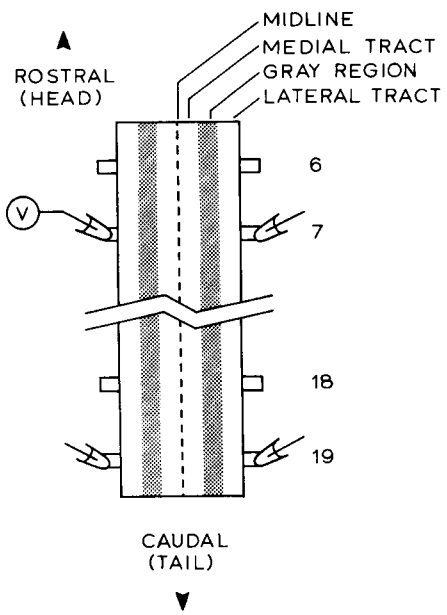

Fig. 1.1. Schematic diagram of visible tracts in spinal cord and recording arrangement

Swimming consists of a sequence of traveling waves which pass down the body and propel the fish through the water. The speed of the fish is a function of the frequency of the traveling waves. In general, over a wide range of frequencies, there is variation neither in the amplitude of the waves nor in the changes of shape undergone by the body. To achieve this movement the electromyographic activity of the myotomal muscle of a fish exhibits a stereotyped temporal pattern (Grillner and Kashin, 1976). The VR output pattern underlying the muscle activity is believed to have three important features: 1) The activity of the two ventral roots of a single segment strictly alternates in time; 2) the duration of the activity of a VR is a constant proportion of the period of the cycle (ca. 40% of the cycle); 3) there is a delay between the bursts of any two ipsilateral ventral roots and that delay is proportional to the period. The third feature implies that the delay occupies a constant phase of the cycle, i.e. there is a constant phase coupling between the two segments. When these features have been demonstrated we can designate a VR discharge pattern as "fictive swimming". This term means that even though the muscles are removed and there is no movement possible, the neural output of the cord is equivalent to that of an intact swimming fish.

To date, a fragment of lamprey spinal cord as short as 4 segments has been observed to generate the swimming pattern as evidenced by recording from its ventral roots (Cohen and Wallén, 1980). (The total cord consists of about 100 segments.) However, a piece of cord containing ten or more segments generally can produce a more stable and regular fictive swimming (Fig. 1.2). The ability to generate the pattern is not a property of any restricted region of the cord. Rather, it appears to be distributed throughout, as any group of segments can produce the pattern.

We have attempted to model the system which provides the intersegmental coordination necessary for maintaining the traveling wave described above. We begin with a model which retains the major characteristics of our system and which is amenable to simple mathematical analysis. Although it represents a drastic simplification of the biology, by adding to or changing elements of this basic model we can begin to determine how the biological analogue of an element may be contributing to the pattern. In our discussion, we assume that each segment of the cord consists of a pair of neural networks which can generate oscillatory activity. Pairs of oscillators are assumed to be coupled together to form the CPG which then

Fig. 1.2. Ventral root recordings from an isolated piece of spinal cord. Recordings are from the right and left roots of segments 7 and 19 (from Cohen and Wallén, 1980)

generates the complete stable pattern. It is possible that a single oscillator is composed of a greater number of segments; it is also possible that there are essential crossed connections between the hemi-segments so that a single oscillator spans the entire segment. The evidence for our basic assumptions is circumstantial (Cohen and Wallén, 1980), as the conclusive tests must await a greater understanding of the cord. However, the form of these assumptions is not critical to the model.

Let us begin by outlining the type of data which our model must encompass. The results are from experiments on isolated spinal cords of silver lampreys (*Icthyomyzon unicuspis*).

When viewed under the dissecting microscope, the cord appears to have three distinct pairs of bands which form the medial fiber tracts, the gray cellular region, and the lateral tracts (Fig. 1.1). Within these three regions small symmetric pairs of transverse lesions were made, cutting across part or all of the fiber tracts. Recordings from VRs rostral and caudal to the lesion(s) were obtained during fictive swimming and compared with recordings made before the lesion. In this way it was possible to determine the changes in coordination resulting from disrupting the pathways. In some cases as a final control, recordings were made after completely severing the cord at the lesion site.

It should be noted that any lesion has a two-fold effect. Some fibers are cut, thereby eliminating their influence. However, the lesion will also unmask the capacity of those fibers which have been left intact. In addition, factors outside the range of the experimenter's control can effect the behavior of the cord.

Often little change was observed after small or even relatively large lesions. This was true regardless of the site of the lesion. Effects on intersegmental coordination were manifest only after the cuts extended over half the width of the cord. Such cuts could include either the complete medial tracts plus part of the medial gray region, or the complete lateral tracts plus part of the lateral gray region. This implies that there are numerous distributed fibers capable of maintaining coordination between segments. However, there is good evidence that the different fiber tracts differ in the strength and the direction of their coupling fibers; a comprehensive study to characterize them is in progress. It is possible to induce clear disturbances in the intersegmental coupling; we will describe the form these disturbances take to allow evaluation of the models presented below.

After a lesion was made and before a cord regained stability many transient phenomena were observed. The most notable example was 2 : 1 bursting of the VRs. That is, the frequency of the bursting in one of the roots was twice the frequency of the root across the lesion. Such activity was followed by both roots stabilizing at a common frequency mid-way between the rates seen during 2 : 1 activity. Bursts of 3 : 1, 4 : 1, etc. were also occasionally observed.

When the cut encompassed almost the entire width of the cord the groups of segments above and below the lesion drifted independently of each other at different frequencies. However, with lesions stopping short of this point, there was evidence of residual interactions conveyed via the intact fiber tracts. In one example (a medial lesion), the frequencies of bursting of the rostral and caudal VRs began independently, but slowly converged to a common frequency where they remained with brief episodes of drifting and locking (Fig. 1.4). In another example (a lateral lesion), the rostral VR was relatively stable while the caudal drifted away and

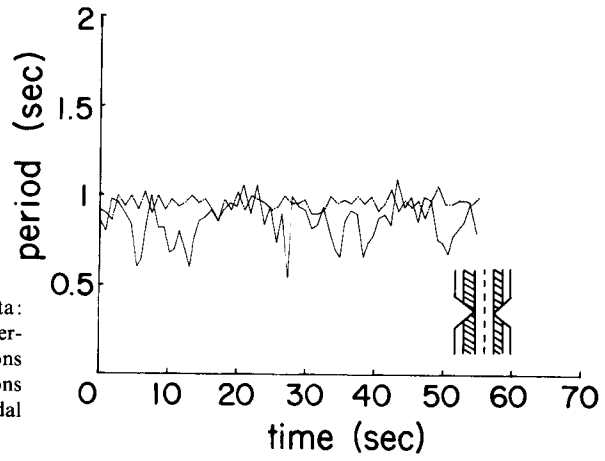

Fig. 1.3. Plot of experimental data: period between successive bursts versus time for a spinal cord with lesions of the lateral tracts and gray regions (medial tracts intact). Rostral, caudal shown dashed, solid respectively

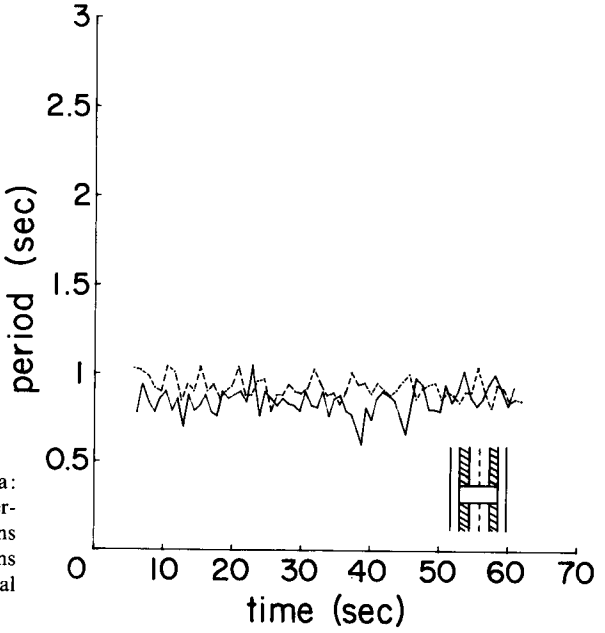

Fig. 1.4. Plot of experimental data: period between successive bursts versus time for a spinal cord with lesions of the medial tracts and gray regions (lateral tracts intact). Rostral, caudal shown dashed, solid respectively

returned to the frequency of the rostral VR (Fig. 1.3). In the latter case after cutting completely through the cord the caudal segments bursted stably at their own frequency, suggesting that the source of their previous disturbance originated rostrally. In both these experiments cutting very few additional fibers removed all interaction. In several other experiments, the regions above and below the cut were reasonably coordinated up to the final cut which then allowed them to drift apart. In several instances, after lateral lesions were made, the caudal segments became less stable than the rostral but their frequencies were the same, making it unclear whether the coordinating system was responsible for the instability.

At the completion of each of four experiments, the cords were cut into three 15 segment pieces. VR recordings from the otherwise identical pieces allowed us to measure the natural frequencies of the three regions. In three of the four cords, the caudal had the highest frequency, middle next and rostral lowest. In the fourth cord the order was reversed, and in several less controlled experiments the rostral segments were also fastest. More experiments are required to determine if these include the complete range of possibilities.

In this paper we shall concentrate on modelling the more general aspects of these particular observations.

2. A Mathematical Model for the Central Pattern Generator

We start by recalling the fundamental characteristics of the intact cord which any model must reproduce:

(a) there is a 180° phase difference between left and right hand roots within individual segments: such intrasegmental locking is apparently stronger than intersegmental coupling,

(b) all segments are (to first order) frequency and phase locked, although variations and "hunting" about equilibrium can occur (Cohen and Wallén, 1980),

(c) there is a phase lag (constant to first order) from head to tail.

On the basis of the experimental evidence summarized in section 1 we make the following assumptions:

Assumption 1 (oscillators). A neuronal oscillator, or pair of oscillators, is associated with each segment. Whether it lies physically within a single segment, or involves essential components which are distributed over several segments, is immaterial to our argument. Each oscillator, in isolation, with the removal of all nonessential interneurons linking it to other segments, exhibits an asymptotically stable periodic oscillation. (Asymptotic stability implies that, after perturbation by external stimuli, the oscillator returns to its stable bursting after a short transient.) Individual oscillator frequencies may vary both absolutely and relative to one another and may be externally influenced (by drug concentration, electrical stimulation, etc.), but their amplitudes are governed primarily by internal factors.

We shall not speculate here on the internal structure of the oscillators, each of which may involve several hundred neurons and necessitate a complex circuit diagram. The description of the neuronal network is under way, but will undoubtedly require many years of experimental effort. Rather, we shall argue that simple phenomenological observations lead to a model which is adequate for our present purpose: that of studying the effects of intersegmental coupling.

Assumption 2 (coupling). Each segmental oscillator or pair of oscillators is coupled to its immediate neighbors and also possibly to distant oscillators. Each oscillator may also be connected to a central "control line" involving certain long axons in the medial tract. (Tonic (constant over time) stimulation of these axons causes uniform frequency changes along the length of the cord (Cohen and Buchanan, 1980).)

Equipped with these reasonable hypotheses, we now formulate a mathematical model which takes the form of a set of N coupled limit cycle oscillators.

The Individual Oscillator or Oscillator Pair

As we have already noted, each oscillator may be distributed over both sides of a segment or over several segments and therefore may involve several hundred neurons. Our key observation is that the membrane potentials of several classes of spinal neurons (Russell and Wallén, 1979; Cohen and Buchanan, 1980), and in particular the ventral root outputs of individual segments, undergo stable periodic variations and thus any dynamical system modelling such a segmental oscillator should have an attracting limit cycle, γ (cf. Pinsker and Bell, 1981). Letting $\mathbf{x} = \mathbf{x}(t) = (x_1(t), x_2(t), \ldots, x_n(t))$ be an n-vector of the relevant variables, a typical model might be an ordinary differential equation of the form

$$\dot{\mathbf{x}} = \mathbf{f}(\mathbf{x}), \tag{2.1}$$

where a dot denotes d/dt. The variables $\mathbf{x}$ could designate, among other things, the periodically varying membrane potentials (including both slow changes as well as action potentials), and the rate of release of neurotransmitter substances. However, since the nature of the oscillator is still unknown, we have chosen to propose a model which does not require detailed specification of the variables $\mathbf{x}$.

Our first important step, which obviates the need for detailed modelling of the function $\mathbf{f}$, is to choose a local coordinate system based on the periodic orbit γ, which forms a closed curve in the state space. Let the *phase*, θ, running from 0 to 2π radians, be measured around γ starting at the point $p \in \gamma$ at which bursting commences, and let the parameterization of γ by θ be chosen such that the speed of the solution is constant with respect to θ. In what follows, remember that θ is taken modulo 2π, so that $\theta = \theta_0 + 2n\pi$ and $\theta = \theta_0$ are equivalent. Let the *amplitude deviation* vector $\mathbf{r}$ represent the remaining $(n-1)$ variables transverse to γ with $\mathbf{r} = 0$ corresponding to points on γ. Provided that γ is smooth, such a local coordinate system can always be chosen (see Fig. 2.1, in which we display the special case $n = 3$).

In terms of this parameterization, (2.1) becomes

$$\dot{\mathbf{r}} = \mathbf{f}_1(\mathbf{r}, \theta), \tag{2.2}$$

$$\dot{\theta} = \omega + f_2(\mathbf{r}, \theta), \tag{2.3}$$

where $\mathbf{f}_1(\mathbf{0}, \theta) = \mathbf{0}$, $f_2(\mathbf{0}, \theta) = 0$ and $T = 2\pi/\omega$ is the period of the oscillator. The functions $\mathbf{f}_1$ and f_2 are necessarily periodic of period 2π with respect to θ. If we further assume that the system is *structurally stable* (cf. Chillingworth, 1976), a reasonable assumption in view of the persistence of stable bursting under a wide range of conditions, then it follows that γ is a *hyperbolic attractor* (Chillingworth, 1976), and all neighboring orbits approach it exponentially fast. Thus, in studying steady solutions in the absence of external excitation, we need merely consider the single scalar *phase equation*

$$\dot{\theta} = \omega, \tag{2.4}$$

with solution

$$\theta(t) = \theta(0) + \omega t. \tag{2.5}$$

We next consider the situation which might be expected to exist within a single segment (or minimal segment set): an opposing pair of strongly coupled oscillators,

linked such that their outputs $\mathbf{x}_L(t)$ and $\mathbf{x}_R(t)$ are 180° (i.e. π radians) out of phase. Taking similar models for each oscillator, we have a coupled pair of equations

$$\dot{\mathbf{x}}_R = \mathbf{f}_R(\mathbf{x}_R, \mathbf{x}_L), \tag{2.6a}$$

$$\dot{\mathbf{x}}_L = \mathbf{f}_L(\mathbf{x}_L, \mathbf{x}_R). \tag{2.6b}$$

To each oscillator we could now associate a phase θ_R, θ_L and a vector $\mathbf{r}_R$, $\mathbf{r}_L$ measuring deviation from its limit cycle. However, rather than two independent frequencies we find evidence of only one, and hence we assume that the constant phase relationship

$$\theta_L(t) = \theta_R(t) + \pi \tag{2.7}$$

holds, at least to first order. This in turn implies that the original variables $\mathbf{x}_R$ and $\mathbf{x}_L$ are also 180° out of phase,

$$\mathbf{x}_L(t) = \mathbf{x}_R(t + T/2), \tag{2.8}$$

where T is the common period. Thus the variables $\mathbf{x}_R$ and $\mathbf{x}_L$ are related and equations (2.6a, b) can be reduced to single equation, say for $\mathbf{x}_R$ or for $\mathbf{r}_R$ and θ_R, and once more we obtain the reduced system (2.2), (2.3).

Phase Variation and Bursting

To relate our simple phase variable model (2.4) to the actual output observed, we note that, as θ increases, the levels of the dynamic variables $\mathbf{x}(t)$ rise and fall periodically. In many models of bursting membranes (e.g. Keener et al., in press; Carpenter, 1979), a *slow* increase in certain variables leads to a triggering of repetitive spikes as a set of *fast* variables change relatively quickly. Typically, all the time for which the slow (driving) variable exceeds some critical threshold level, spikes occur. In the present system the state of an oscillator is best reflected by the rhythmic changes in membrane potential of motoneurons. The output from the oscillator, as observed in the motoneuron, varies relatively smoothly. If the input depolarizes the membrane potential beyond threshold, the cell fires a burst of action potentials (Fig. 1.2). Let us suppose that triggering occurs for $\theta = 0$ (at the point p on γ) and ceases for $\theta = \hat{\theta}$ ($\approx 2\pi \times 0.4$, from observations). Then a typical slow variable $x(t)$ and the spike output appear as shown in Fig. 2.2. In this paper we are not concerned with spike generation as such, but rather with the phase relationships

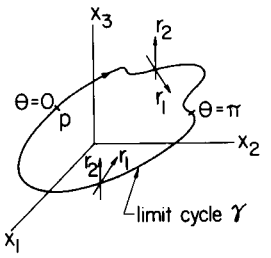

2.1

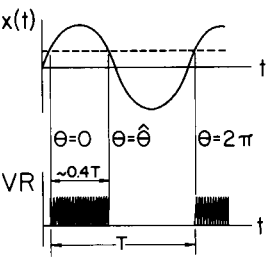

2.2

Fig. 2.1. The phase space of Eq. (2.1) in the special case $n = 3$, for which $\mathbf{r}$ is a 2-vector, $\mathbf{r} = (r_1, r_2)$

Fig. 2.2. The oscillator output $x(t)$ and its relation to the ventral root output *VR*. The threshold level is shown as a *dashed line*

between the slow driving signals, and thus we do not further discuss the rapid potential changes involved in spike generation.

The Chain of Oscillators

Continuing our analysis as above we write N equations of the form (2.1) for the N oscillators, a typical member of the set being

$$\dot{\mathbf{x}}_j = \mathbf{f}_j(\mathbf{x}_j) + \mathbf{g}_j(\mathbf{x}_1, \ldots, \mathbf{x}_N, \boldsymbol{\alpha}), \qquad j = 1, \ldots, N, \tag{2.9}$$

where $\mathbf{g}$ is the coupling function, involving the dynamics of the other $N-1$ oscillators, and including a vector of coupling coefficients, $\boldsymbol{\alpha}$. When $\boldsymbol{\alpha} = \mathbf{0}$, $\mathbf{g}_j(\mathbf{x}_1, \ldots, \mathbf{x}_N, \mathbf{0}) = \mathbf{0}$ and we have N independent oscillators, each exhibiting a stable limit cycle γ_j.

To proceed, we assume that the coupling is relatively weak, so that $|\boldsymbol{\alpha}|$ is small and $|\mathbf{g}| \ll |\mathbf{f}|$. In such a case the limit cycles of the uncoupled oscillators are each slightly perturbed and one can continue to use the phase coordinates θ_j, and amplitude deviations $\mathbf{r}_j$ to characterize the state of each oscillator. In this way one obtains sets of equations of the form

$$\begin{aligned} \dot{\mathbf{r}}_j &= \mathbf{f}_{j1}(\mathbf{r}_j, \theta_j) + \mathbf{g}_{j1}(\mathbf{r}_1, \ldots, \mathbf{r}_N, \theta_1, \ldots, \theta_N, \boldsymbol{\alpha}), \\ \dot{\theta}_j &= \omega_j + f_{j2}(\mathbf{r}_j, \theta_j) + g_{j2}(\mathbf{r}_1, \ldots, \mathbf{r}_N, \theta_1, \ldots, \theta_N, \boldsymbol{\alpha}), \\ j &= 1, 2, \ldots, N \end{aligned} \tag{2.10}$$

which of course reduce to (2.2), (2.3) when $\boldsymbol{\alpha} = 0$. Here the individual uncoupled oscillators may each have different periods, $T_j = 2\pi/\omega_j$, as experiments with completely severed cords indicate. Expanding equations (2.10) about $\mathbf{r}_j = 0$ in Taylor series, one eventually obtains approximate phase equations for weakly coupled oscillators in the form

$$\dot{\theta}_j = \omega_j + h_j(\theta_1, \ldots, \theta_N, \boldsymbol{\alpha}), \qquad j = 1, \ldots, N \tag{2.11}$$

from which all the amplitudes are absent (cf. Holmes, 1980; Rand and Holmes, 1980; Cohen and Neu, 1979; Neu, 1979, 1980a, b; Ermentrout, 1981).

In our case the observation that periodic bursting occurs both in intact and (moderately) lesioned cords indicates that, uncoupled or even *strongly* coupled, each oscillator during steady running is performing a limit cycle oscillation and this can still be characterized in terms of its phase θ_j. Since the primary aspect of coupling is to fix phase relationships we are again led to a phase coupling model of the form (2.11).

So far we have reduced a system of N or $2N$ segmental oscillators, each governed by a set of differential equations, to a system of N phase equations. We now ask what form might the functions h_j be expected to take. A linear coupling model might be a reasonable candidate. For such a model, in terms of the original variables, the effect of coupling on the ith oscillator by the jth oscillator is proportional to $\mathbf{x}_j$: a system of coupled oscillators would obey

$$\dot{\mathbf{x}}_i = \mathbf{f}_i(\mathbf{x}_i) + \sum_{j=1}^{N} \mathbf{A}_{ij}\mathbf{x}_j, \tag{2.12}$$

where $\mathbf{A}_{ij}$ are matrices of coupling coefficients multiplying the vectors $\mathbf{x}_j$.

It has been shown (Rand and Holmes, 1980; Neu, 1980a, b) that in the case of weak coupling such a system leads to the following phase equations

$$\dot{\theta}_i = \omega_i + \sum_{j=1}^{N} \alpha_{ij} h(\theta_j - \theta_i), \tag{2.13}$$

where h is a bounded periodic function of its argument.

The simplest periodic function, $h(\phi) = \sin\phi$, arises in cases in which the unperturbed uncoupled limit cycles are sinusoidal. It turns out that this simple choice leads to a model which readily reproduces many of our experimental observations, and thus we will pursue it further in the following sections. We cite as further evidence in its support typical observations which indicate that the slowly varying intracellular potentials of motoneurons are quasi-sinusoidal in nature (Cohen and Buchanan, 1980).

It is of interest to compare these assumptions regarding coupling to the results of phase response curve (PRC) experiments. In these experiments an electrical stimulus is suddenly applied to one oscillator and its effect on another oscillator is observed. Typical PRC's (Pavlidis, 1973; Stein, 1976) show that the effect of a small disturbance is smallest when the disturbance occurs near $\theta = 0$, and is greatest when it occurs near $\theta = \pi$, Fig. 2.3. Stimulation experiments on the lamprey spinal cord also generate data exhibiting the discontinuous ramp function of Fig. 2.3 (unpublished observation, Cohen and Wallén). Now our model has been chosen such that the effect of an oscillator j on an oscillator i is zero when they are in phase ($\phi = 0$) and greatest when they are $\pi/2$ out of phase ($\phi = \pm \pi/2$), cf. Fig. 2.3. The choice $h(\phi) = \sin\phi$ can be thought of as an approximation to the discontinuous ramp function of Fig. 2.3, representing typical PRC data. (E.g. the PRC function could be expanded in a Fourier series, since it is necessarily periodic. If the series is truncated after one term, we obtain the model considered in this paper.)

In this way we arrive at a set of N coupled equations for the phases of the oscillators:

$$\dot{\theta}_i = \omega_i + \sum_{j=1}^{N} \alpha_{ij} \sin(\theta_j - \theta_i). \tag{2.14}$$

Here α_{ij} represents the strength of the coupling effect of the jth oscillator on the ith oscillator, a *positive* sign indicating *excitatory* coupling (θ_j tends to pull θ_i towards it) and a *negative* sign indicating *inhibitory* coupling (θ_j tends to push θ_i away from it). A schematic representation of this system is shown in Fig. 2.4.

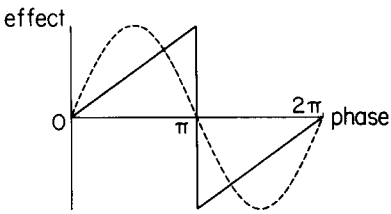

2.3

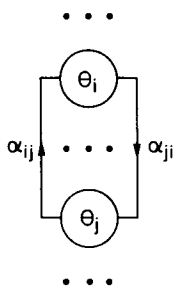

2.4

Fig. 2.3. Comparison of our assumed coupling function $h(\phi) = \sin\phi$ (*shown dashed*) with typical PRC data (*shown solid*)

Fig. 2.4. Schematic representation of the system of Eq. (2.14)

In Eqs. (2.14) the relative magnitudes of ω_i and α_{ij} are assumed to be such that $\theta_i(t)$ is a monotone increasing function of t for all initial conditions, i.e. such that $\dot{\theta}_i$ never vanishes. This means that the uncoupled motion around the limit cycle γ is preserved under the coupling in the sense that no motion can stop and reverse the direction of its flow around γ.

In the next section we show that simple models of the type derived above provide reasonable descriptions of much of the observed behavior of both intact and lesioned cords.

3. Analysis of the Mathematical Model

We first consider some simple models, the solutions of which provide traveling waves with phase lags between segments such as those observed in the intact fish. We find that such solutions can arise in the case of nearest neighbor coupling with detuning of oscillators, as well as in the case of long distance coupling combined with nearest neighbor coupling. We then consider the loss of coupling and the onset of drift in order to relate our model to the lesion experiments.

Nearest Neighbor Coupling

The simplest model is one in which each oscillator is coupled only to its nearest neighbors and (2.14) takes the form

$$\begin{aligned}
\dot{\theta}_1 &= \omega_1 + \alpha_{12}\sin(\theta_2 - \theta_1),\\
\dot{\theta}_2 &= \omega_2 + \alpha_{21}\sin(\theta_1 - \theta_2) + \alpha_{23}\sin(\theta_3 - \theta_2),\\
&\cdots\\
\dot{\theta}_j &= \omega_j + \alpha_{j,j-1}\sin(\theta_{j-1} - \theta_j) + \alpha_{j,j+1}\sin(\theta_{j+1} - \theta_j),\\
&\cdots\\
\dot{\theta}_N &= \omega_N + \alpha_{N,N-1}\sin(\theta_{N-1} - \theta_N).
\end{aligned} \tag{3.1}$$

Letting $\phi_j = \theta_j - \theta_{j+1}$ and $\Omega_j = \omega_j - \omega_{j+1}$ and subtracting pairwise, we obtain a set of $N-1$ equations for the phase differences ϕ_j, $j = 1, \ldots, N-1$.

$$\begin{aligned}
\dot{\phi}_1 &= \Omega_1 - (\alpha_{12} + \alpha_{21})\sin\phi_1 + \alpha_{23}\sin\phi_2,\\
\dot{\phi}_2 &= \Omega_2 + \alpha_{21}\sin\phi_1 - (\alpha_{23} + \alpha_{32})\sin\phi_2 + \alpha_{34}\sin\phi_3,\\
&\cdots\\
\dot{\phi}_j &= \Omega_j + \alpha_{j,j-1}\sin\phi_{j-1} - (\alpha_{j,j+1} + \alpha_{j+1,j})\sin\phi_j + \alpha_{j,j+1}\sin\phi_{j+1},\\
&\cdots\\
\dot{\phi}_{N-1} &= \Omega_{N-1} + \alpha_{N-1,N-2}\sin\phi_{N-2} - (\alpha_{N-1,N} + \alpha_{N,N-1})\sin\phi_{N-1}.
\end{aligned} \tag{3.2}$$

If we further assume that all upward coupling strengths $\alpha_{j,j+1}$ are equal to α_u and all downward strengths $\alpha_{j,j-1}$ are equal to α_d, this becomes

$$\dot{\boldsymbol{\phi}} = \boldsymbol{\Omega} + \mathbf{B}\mathbf{S}, \tag{3.3}$$

where

$$\boldsymbol{\phi} = \begin{bmatrix} \phi_1 \\ \vdots \\ \phi_{N-1} \end{bmatrix}, \quad \mathbf{S} = \begin{bmatrix} \sin\phi_1 \\ \vdots \\ \sin\phi_{N-1} \end{bmatrix}, \quad \boldsymbol{\Omega} = \begin{bmatrix} \Omega_1 \\ \vdots \\ \Omega_{N-1} \end{bmatrix}, \tag{3.4}$$

are $N-1$ vectors and

$$\mathbf{B} = \begin{bmatrix} -(\alpha_d + \alpha_u) & \alpha_u & & \\ \alpha_d & -(\alpha_d + \alpha_u) & \alpha_u & \\ & & \cdots & \\ & & \alpha_d & -(\alpha_d + \alpha_u) \end{bmatrix} \tag{3.5}$$

is a tri-diagonal $(N-1) \times (N-1)$ matrix. We shall be especially interested in 1 : 1 phase locked solutions of (3.1), in which all oscillators exhibit the same frequency. Henceforth such solutions will simply be called "phase locked", and "drifting" will denote the absence of 1 : 1 phase locking, which does not preclude m/n phase locking for $m, n \neq 1$. (Here we do not wish to consider these more delicate situations, cf. Ermentrout, 1981.) If any phase locked solutions exist they are given by the equilibria of (3.3), the roots of

$$\mathbf{S} = -\mathbf{B}^{-1}\boldsymbol{\Omega}, \tag{3.6}$$

Clearly no such solutions exist if any element of $\mathbf{B}^{-1}\boldsymbol{\Omega}$ has magnitude greater than one.

As an example, for a system of two oscillators one obtains the single phase difference equation for $\phi = \theta_1 - \theta_2$

$$\dot{\phi} = \Omega - (\alpha_d + \alpha_u)\sin\phi, \tag{3.7}$$

which has phase locked solutions if and only if

$$|\Omega| \leqslant |\alpha_d + \alpha_u|. \tag{3.8}$$

Linearization reveals that there is one degenerate (semi-stable) solution $\phi_1 = \pi/2$ (resp. $3\pi/2$) for $|\Omega| = |\alpha_d + \alpha_u|$ and a pair of solutions, one stable and the other unstable, for $|\Omega| < |\alpha_d + \alpha_u|$. Thus, as the coupling strength $|\alpha_d + \alpha_u|$ decreases relative to the detuning $\Omega = \omega_1 - \omega_2$ a *bifurcation* occurs in which the stable phase locked solution coalesces with the unstable one and vanishes, cf. Fig. 3.1. We shall subsequently study the dynamics of transient (non-steady) solutions near this point.

For three oscillators equation (3.6) becomes

$$\begin{bmatrix} \sin\phi_1 \\ \sin\phi_2 \end{bmatrix} = \frac{1}{\alpha_d^2 + \alpha_d\alpha_u + \alpha_u^2} \begin{bmatrix} \alpha_d + \alpha_u & \alpha_u \\ \alpha_d & \alpha_d + \alpha_u \end{bmatrix} \begin{bmatrix} \Omega_1 \\ \Omega_2 \end{bmatrix}, \tag{3.9}$$

which reduces to

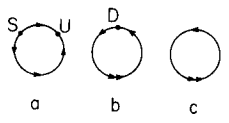

Fig. 3.1. The disappearance of phase locked solutions as $|\alpha_d + \alpha_u|$ decreases relative to $|\Omega|$. (In this Fig. Ω and $\alpha_d + \alpha_u$ have been taken positive.) **a, b, c** correspond respectively to $|\Omega|$ less than, equal to, and greater than $|\alpha_d + \alpha_u|$. S = stable, U = unstable, D = degenerate. See Rand and Holmes, 1980

$$\sin\phi_1 = (2\Omega_1 + \Omega_2)/3\alpha, \qquad \sin\phi_2 = (\Omega_1 + 2\Omega_2)/3\alpha \tag{3.10}$$

if $\alpha_u = \alpha_d = \alpha$. Thus stable phase locking occurs if and only if

$$\max\{|2\Omega_1 + \Omega_2|, |\Omega_1 + 2\Omega_2|\} < |3\alpha|. \tag{3.11}$$

Computations for longer chains of oscillators rapidly become awkward and a better approach is to insert the observed phase locked and lagged solution into (3.3) or (3.6) and thus calculate appropriate parameter values for its realization. In this way we find that a *constant* identical segment to segment phase lag of $\theta_j - \theta_{j+1} = \phi_j = \delta$, characteristic of a uniform traveling wave, is easily achieved by detuning the rostral (θ_1) and caudal (θ_N) oscillators only. We require

$$\begin{aligned}
\Omega_1 + [-(\alpha_d + \alpha_u) + \alpha_u]\Delta &= 0,\\
&\vdots\\
\Omega_j + [\alpha_d - (\alpha_d + \alpha_u) + \alpha_u]\Delta &= 0,\\
&\vdots\\
\Omega_{N-1} + [\alpha_d - (\alpha_d + \alpha_u)]\Delta &= 0,
\end{aligned} \tag{3.12}$$

where $\Delta = \sin\delta > 0$. This implies that $\Omega_j = 0$ for $j = 2, \ldots, N-2$ and $\Omega_1 = \alpha_d\Delta$, $\Omega_{N-1} = \alpha_u\Delta$, or

$$\begin{aligned}
&\omega_j = \omega \qquad \text{for all} \qquad j \neq 1, N,\\
&\omega_1 = \omega + \alpha_d \sin\delta > \omega,\\
&\omega_N = \omega - \alpha_u \sin\delta < \omega.
\end{aligned} \tag{3.13}$$

Here the overall frequency ω, is also the common natural (isolated) frequency of the central portion of the cord, while the caudal oscillator is tuned down and the rostral oscillator tuned up. Here we assume that the coupling α_d, $\alpha_u > 0$ is excitatory.

To study the stability of this solution we linearize (3.3) about the fixed point $\phi_j = \sin\delta$ to obtain

$$\dot{\xi} = \mathbf{B}'\xi,$$

where $\mathbf{B}' = \mathbf{B}\cos\delta$. If, as is the case in our observations, δ is a small angle, so that $0 < \cos\delta < 1$, it can be shown that all eigenvalues of $\mathbf{B}'$ have negative real parts and thus that the uniform phase lagged solution is asymptotically stable. There are, of course many other solutions, since there are two roots of each equation $\sin\phi_j = \Delta$, leading to a total of 2^{N-1} phase locked solutions. However, linearizations and calculations such as that above reveal that all the other solutions are unstable.

We conclude that, if nearest neighbor coupling predominates, and the rostral oscillator runs appreciably faster, and the caudal oscillator appreciably slower than the central portion of the cord, then stable traveling wave solutions result. We note that since each of the 2^{N-1} phase locked periodic orbits corresponds to a hyperbolic fixed point, the system is structurally stable (Chillingworth, 1976) and hence can be expected to persist under small perturbations, such as the addition of weak long distance coupling and slightly irregular frequency modulation. Of course, if the detuning is irregular, with a general tendency for frequency decrease from head to tail, then less uniform phase lags are produced. We note that if all the

oscillators are identical ($\Omega_j = 0, \forall_j$) then no phase lag is possible and the only stable solution is $\phi_j \equiv 0$ for all j. Similarly if the caudal oscillator is tuned up and the rostral oscillator tuned down then a traveling wave propagates from tail to head.

An alternate approach to assuming a constant phase lag δ is to take each oscillator's frequency ω_j to be smaller than its predecessor's, ω_{j-1}, by a fixed amount ε,

$$\omega_j = \omega_{j-1} - \varepsilon, \qquad j = 2, \ldots, N$$

i.e.

$$\omega_j = \omega_1 - (j-1)\varepsilon, \qquad j = 1, \ldots, N,$$

whereupon a *nonuniform* phase locked solution can be found (if ε is small enough), i.e. the phase difference $\phi_j = \theta_j - \theta_{j+1}$ will depend on the position j. This may be demonstrated in the case of N oscillators with equal coupling $\alpha_{ij} = \alpha$ (i.e. $\alpha_u = \alpha_d = \alpha$ in Eq. (3.5)), as follows: We invert the $(N-1) \times (N-1)$ matrix $\mathbf{B}$ of Eq. (3.5),

$$\mathbf{B} = \alpha \begin{bmatrix} -2 & 1 & & & & \\ 1 & -2 & 1 & & & \\ & & \cdots & & & \\ & & & 1 & -2 & 1 \\ & & & & 1 & -2 \end{bmatrix}$$

obtaining a symmetric inverse $\mathbf{B}^{-1}$ with elements

$$(\mathbf{B}^{-1})_{ij} = (\mathbf{B}^{-1})_{ji}, \qquad i,j = 1, \ldots, N-1,$$

where

$$(\mathbf{B}^{-1})_{ij} = \frac{j(N-i)}{-N} \qquad (i \geqslant j).$$

Then substituting into (3.6) with the $N-1$ vector

$$\mathbf{\Omega} = \varepsilon \begin{bmatrix} 1 \\ 1 \\ 1 \\ \cdots \\ 1 \end{bmatrix}$$

we find

$$\sin \phi_j = \frac{\varepsilon}{\alpha} \frac{j}{2}(N-j), \qquad j = 1, \ldots, N-1. \tag{3.14}$$

In order for there to exist roots ϕ_i we require that

$$\varepsilon \leqslant \frac{8}{N^2}\alpha.$$

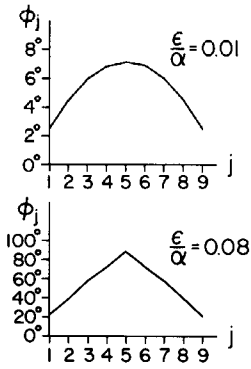

Fig. 3.2. Plot of ϕ_j versus j for a system of 10 oscillators with $\Omega = (\varepsilon, \varepsilon, \ldots, \varepsilon)$

Equation (3.14) may be displayed by plotting ϕ_j against j. For example in the case of $N = 10$ oscillators, Fig. 3.2 shows such plots for various values of ε/α.

By using Eq. (3.14) we may calculate the phase angle θ_j for each oscillator, $j = 2, \ldots, N$, relative to the (arbitrary) phase angle θ_1 of oscillator 1:

$$\theta_j = \theta_1 - \sum_{k=1}^{j-1} \phi_k, \qquad j = 2, \ldots, N.$$

In order to conveniently display these results, we will plot $\sin\theta_j$ against j. For example, in the case of $N = 10$ oscillators, Fig. 3.3 shows such plots for various values of ε/α when $\theta_1 = 0$. Although these graphs remind us of the shape of a swimming fish, biomechanical factors could complicate the precise relationship between the activity of the motoneurons and the overall shape of the fish.

We note that Grasman and Jansen, 1980, and Linkens, 1974, 1976, found similar traveling wave solutions in one and two dimensional arrays of coupled relaxation and van der Pol oscillators.

We end by noting that occasionally a central segment was observed to take the lead. The present model easily accounts for this by assuming that one oscillator (say the kth), is tuned appreciably above the others, so that

$$\omega_k > \omega_1 = \omega_2 = \cdots = \omega_{k-1} = \omega_{k+1} = \cdots = \omega_n = \omega$$

and thus $\Omega_j = 0$, $j = 1, \ldots, k-2, k+1, \ldots, N-1$, while $\Omega_{k-1} < 0 < \Omega_k$. Performing an analysis similar to that above we find that a traveling wave propagates both rostrally and caudally from the kth segment. These same conclusions would also hold in the case that $N - 1$ of the oscillators have nearly (but not exactly) the same frequencies ω_i.

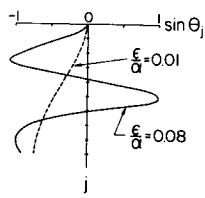

Fig. 3.3. Plot of $\sin\theta_j$ versus j for a system of 10 oscillators with $\Omega = (\varepsilon, \varepsilon, \ldots, \varepsilon)$. Here θ_1 has been taken as zero

Three and N Oscillators With Long Distance Coupling

The study of general coupled systems of the form (2.13) is intractible analytically and computer solutions must be sought. It is therefore worth carrying out studies of special cases such as those above and the present one. Here we take three oscillators, with identical nearest neighbor coupling coefficients α, and distant coupling β between oscillators 1 and 3, Fig. 3.4.

The appropriate differential equations are

$$\begin{aligned}\dot{\theta}_1 &= \omega_1 + \alpha\sin(\theta_2 - \theta_1) + \beta\sin(\theta_3 - \theta_1),\\ \dot{\theta}_2 &= \omega_2 + \alpha\sin(\theta_1 - \theta_2) + \alpha\sin(\theta_3 - \theta_2),\\ \dot{\theta}_3 &= \omega_3 + \alpha\sin(\theta_2 - \theta_3) + \beta\sin(\theta_1 - \theta_3).\end{aligned} \tag{3.15}$$

We first note that, if a phase locked solution exists, then $\dot{\theta}_1 = \dot{\theta}_2 = \dot{\theta}_3$ and the frequency ($\bar{\omega}$) of this solution, obtained after a little algebraic manipulation, is

$$\bar{\omega} = \frac{\omega_1 + \omega_2 + \omega_3}{3}; \tag{3.16}$$

i.e. the symmetric coupling does not weight any particular oscillator (compare Eq. (3.15) with Eq. (2.14) above). We next let $\phi_1 = \theta_1 - \theta_2$, $\phi_2 = \theta_2 - \theta_3$ and subtract the components of (3.15) pairwise to obtain

$$\begin{aligned}\dot{\phi}_1 &= \Omega_1 - 2\alpha\sin\phi_1 + \alpha\sin\phi_2 - \beta\sin(\phi_1 + \phi_2)\\ \dot{\phi}_2 &= \Omega_2 + \alpha\sin\phi_1 - 2\alpha\sin\phi_2 - \beta\sin(\phi_1 + \phi_2).\end{aligned} \tag{3.17}$$

To seek solutions we first set $\Omega_1 = \Omega_2 = 0$ ($\omega_1 = \omega_2 = \omega_3$, identical oscillators). In this case (3.17) has either four or six fixed points, see Table 1. For this tabulation we again assume that $\alpha > 0$ (excitatory nearest neighbor coupling), but

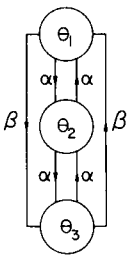

Fig. 3.4. Schematic representation of three oscillators with nearest neighbor and long distance coupling

Table 1. Phase locked solutions of Eq. (3.17) with $\Omega_1 = \Omega_2 = 0$

$\lvert\beta\rvert < \alpha/2$	$(0,0)$ – sink; $(\pi,0)$, $(0,\pi)$ – saddles; (π,π) – source
$\beta > \alpha/2$	$(0,0)$ – sink; $(\pi,0)$, $(0,\pi)$, (π,π) – saddles; $\left(\cos^{-1}\left(\frac{-\alpha}{2\beta}\right), \cos^{-1}\left(\frac{-\alpha}{2\beta}\right)\right)$ – sources
$\beta < -\alpha/2$	$(0,0)$, $(\pi,0)$, $(0,\pi)$ – saddles; (π,π) – sources; $\left(\cos^{-1}\left(\frac{-\alpha}{2\beta}\right), \cos^{-1}\left(\frac{-\alpha}{2\beta}\right)\right)$ – sinks

that β can take either sign. Since the analysis is similar to the cases given above we do not give the details, other than to note that the symmetry of (3.17) with $\Omega_1 = \Omega_2 = 0$ implies that the line $\phi_1 = \phi_2$ is invariant and that the additional pairs of fixed points appearing for $|\beta| > \alpha/2$ are found by setting $\phi_1 = \phi_2 = \phi$ and seeking solutions of

$$-2\alpha \sin\phi + \alpha \sin\phi - \beta \sin 2\phi = 0$$

or

$$\sin\phi(2\beta\cos\phi + \alpha) = 0. \tag{3.18}$$

We see that, if $\beta < -\alpha/2$, corresponding to relatively strong, inhibitory coupling between oscillators 1 and 3, then two stable solutions corresponding to phase lagged (forward) and phase leading (backward) traveling waves appear, with $\phi_j = \theta_j - \theta_{j+1} = \cos^{-1}(-\alpha/2\beta)$, while the in phase solution ($\phi_j = 0$) becomes unstable. Uniform detuning $\Omega_1 = \Omega_2 = \Omega \neq 0$ shifts these solutions as indicated in the bifurcation diagram of Fig. 3.5.

Passing to the case of N oscillators with only the first and last coupled at long distance, again with strength β, and the central ones coupled to nearest neighbors alone, we obtain, for the case of identical oscillators ($\Omega_j = 0$)

$$\begin{aligned}
-2\alpha \sin\phi_1 + \alpha \sin\phi_2 - \beta \sin\left(\sum_{k=1}^{N-1} \phi_k\right) &= 0, \\
&\vdots \\
\alpha \sin\phi_{j-1} - 2\alpha \sin\phi_j + \alpha \sin\phi_{j+1} &= 0, \\
&\vdots \\
\alpha \sin\phi_{N-2} - 2\alpha \sin\phi_{N-1} - \beta \sin\left(\sum_{k=1}^{N-1} \phi_k\right) &= 0.
\end{aligned} \tag{3.19}$$

Thus we find that traveling wave solutions with phase lag $\phi_j = \bar{\phi}$, representing both forward and backward going waves, are possible for values of α, β for which

$$\beta \sin[(N-1)\bar{\phi}] + \alpha \sin\bar{\phi} = 0$$

has nontrivial solutions.

In particular, from Fig. 3.5, the model exhibits, for all Ω, stable forward running phase locked solutions when the long distance coupling is inhibitory and sufficiently strong for a given excitatory nearest neighbor coupling ($-\beta \gg \alpha > 0$).

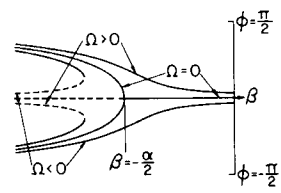

Fig. 3.5. Bifurcation diagram showing the variation of equilibrium solutions $\phi = \phi_1 = \phi_2$ of Eq. (3.17) with β. *Solid lines* are stable, *dashed lines* are unstable

Thus even when the caudal oscillator runs fastest, stable forward running phase locked motions are possible, in accordance with some of our observations. But note that these motions coexist with stable backward running waves, which have not been observed in the isolated cord, although they are exhibited by intact fish.

We conclude that chains of identical oscillators with nearest neighbor coupling plus direct rostral-caudal inhibitory coupling can also exhibit traveling waves of the type observed, although such stable waves appear in pairs, with both forward and backward going waves. We remark that while lampreys are known to have the ability to swim backwards, in almost all cases of stable fictive swimming observed in our in vitro preparations forward traveling waves with the rostral part leading are observed. Frequently in the fictively swimming dogfish (Grillner, 1975) and occasionally in an isolated lamprey spinal cord, one of the central oscillators will take the lead, a phenomenon for which this model with long distance coupling cannot account (although the model with nearest neighbor coupling, Eq. (3.12), can exhibit this behavior).

Transients, Loss of Locking and Drifting with Weak Coupling

An alternative approach to considering the phase locked solutions of N coupled oscillators is to consider the general (not necessarily phase locked) behavior of a smaller system of, say, two oscillators. In applying this kind of study to the fish we must think of "lumping" the many oscillators found in the spinal cord into two groups, each with an average or representative frequency and phase. This approach will be particularly useful in studying the model's predictions regarding the effects of lesions made surgically on a living spinal cord, in which case the two groups of oscillators may be naturally identified with those segments located above and below the lesion site. The effect of the lesion will then be to change the nature of the coupling between the two groups of oscillators. In this application we assume that each group of oscillators stays nearly phase locked relative to the other members of the same group, but that due to the lesion the rostral and caudal groups of oscillators can become uncoupled to an extent dependent upon the nature of the lesion.

The differential equations describing a system of two oscillators are (Fig. 3.6)

$$\dot{\theta}_1 = \omega_1 + \alpha_u \sin(\theta_2 - \theta_1), \tag{3.20}$$

$$\dot{\theta}_2 = \omega_2 + \alpha_d \sin(\theta_1 - \theta_2). \tag{3.21}$$

Subtracting Eq. (3.21) from (3.20), we again obtain Eq. (3.7)

$$\dot{\phi} = \Omega - k \sin \phi, \tag{3.7}$$

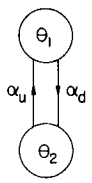

Fig. 3.6. Schematic representation of a system of two oscillators

where

$$\phi = \theta_1 - \theta_2 = \text{phase difference},$$
$$\Omega = \omega_1 - \omega_2 = \text{frequency difference},$$
$$k = \alpha_u + \alpha_d = \text{net coupling}.$$

As discussed above (Eq. (3.8)), this system exhibits a stable phase locked solution if $|k| \geqslant |\Omega|$, i.e. if the net coupling k is strong enough (Fig. 3.1).

However, if the net coupling k is weak, $|k| < |\Omega|$, e.g. due to a lesion, then no phase locked solutions occur. Rather each of the two oscillators "drifts" in a manner which can be investigated by solving Eqs. (3.20), (3.21) exactly, as follows: First we solve (3.7) by separating variables,

$$t = \int \frac{d\phi}{\Omega - k \sin \phi} = \frac{2}{\rho} \arctan\left(\frac{\Omega}{\rho} \tan\frac{\phi}{2} - \frac{k}{\rho}\right) + \text{constant}, \tag{3.22}$$

where $\rho^2 = \Omega^2 - k^2$.

Solving (3.22) for the phase difference $\phi(t)$, we find

$$\phi = 2 \arctan u, \tag{3.23}$$

where

$$u = \frac{k}{\Omega} + \frac{\rho}{\Omega} \tan\left(\frac{\rho t}{2} + C\right),$$

C = arbitrary constant.

In order to solve for the phases $\theta_i(t)$ of the two oscillators, we select C so that at $t = 0$, $\phi(0) = \theta_1(0) - \theta_2(0)$,

$$C = \arctan\left[-\frac{k}{\rho} + \frac{\Omega}{\rho} \tan\left(\frac{\theta_1(0) - \theta_2(0)}{2}\right)\right] \tag{3.24}$$

and substitute (3.23) into (3.20), (3.21). Integrating (3.20), (3.21) from 0 to t gives

$$\theta_1(t) = \omega_1 t + \theta_1(0) - \alpha_u \int_0^t \sin \phi(t)\, dt,$$
$$\theta_2(t) = \omega_2 t + \theta_2(0) + \alpha_d \int_0^t \sin \phi(t)\, dt. \tag{3.25}$$

It remains to evaluate the integral in Eqs. (3.25):

$$\int \sin \phi(t)\, dt = \int \frac{2u}{1+u^2}\, dt, \qquad \text{from (3.23)},$$
$$= \int \frac{2u}{1+u^2} \frac{dt}{du}\, du, \qquad \text{by the chain rule},$$
$$= \frac{4\Omega}{\rho^2} \int \frac{u\, du}{(1+u^2)(1+f^2)}, \qquad \text{from (3.22)},$$
$$= -\frac{2}{k} \int \frac{du}{1+u^2} + \frac{2\Omega}{\rho k} \int \frac{df}{1+f^2},$$

where $f = (\Omega u - k)/\rho$. The evaluation of these last integrals gives

$$\int_0^t \sin\phi(t)\,dt = \frac{\Omega}{k}t - \frac{2}{k}\arctan\left\{\frac{k}{\Omega} + \frac{\rho}{\Omega}\tan\left(\frac{\rho t}{2} + C\right)\right\} + \frac{\theta_1(0) - \theta_2(0)}{k}. \quad (3.26)$$

Substitution of (3.26), (3.24) into (3.25) completely specifies $\theta_i(t)$, $i = 1, 2$.

These results of our model concerning drifting in a system of two oscillators may be considered by graphically displaying the periods of oscillation associated with Eq. (3.25). For this purpose we will plot period (i.e. time between successive occurrences of $\theta_j = 0$) against time for each oscillator. For illustration we shall choose $T_1 = 1$, $T_2 = 1.5$ to be the periods of the completely uncoupled oscillators (i.e., $\omega_1 = 2\pi$, $\omega_2 = 4\pi/3$).

In the phase locked case, Eq. (3.8), the steady state behavior involves both oscillators running at the same frequency, $\omega_1 - \alpha_u\Omega/k = \omega_2 + \alpha_d\Omega/k$, cf. Eqs. (3.20), (3.21), Fig. 3.7. In the case of zero coupling, $\alpha_u = \alpha_d = 0$, the two oscillators run independently at their respective uncoupled frequencies ω_1, ω_2, Fig. 3.8.

The minimum value of $|\alpha_u + \alpha_d|$ required for phase locking turns out to be 2.094...,

$$|\alpha_u + \alpha_d| = \Omega = \omega_1 - \omega_2 = 2\pi/3 = 2.094\ldots.$$

If the coupling is decreased from this value to zero, the behavior of the successive periods of each of the oscillators exhibits certain general characteristics, Figs. 3.9 – 3.14. E.g. for $\alpha_u = \alpha_d = 1.04$ both oscillators exhibit nearly the same frequency of oscillation for most of the time, with regular deviations to uncoupled frequencies (Fig. 3.9). When α_u and α_d are decreased to 1, the proportion of time for which both oscillators have nearly the same frequency is diminished (Fig. 3.10). This illustrates

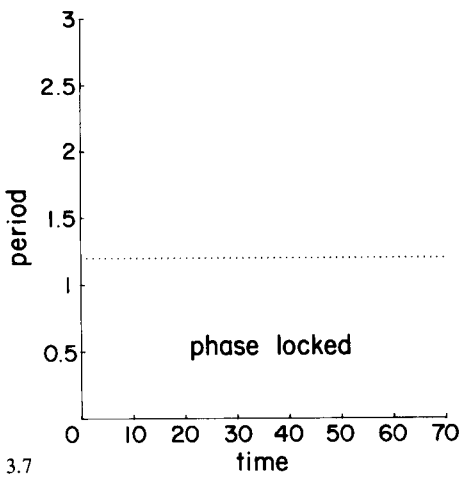

3.7

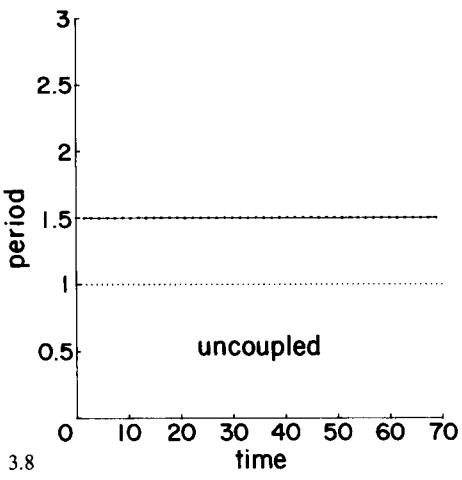

3.8

Fig. 3.7. Behavior of two oscillator model: period versus time plot for phase locked case, $\alpha_u = \alpha_d$, $|\alpha_u + \alpha_d| > 2\pi/3$. Both oscillators are frequency locked with period 6/5

Fig. 3.8. Behavior of two oscillator model: period versus time plot for uncoupled case, $\alpha_u = \alpha_d = 0$. Both oscillators run independently with periods 1, 3/2 respectively. In Figs. 3.8 – 3.14 oscillator no. 1 is shown dashed and oscillator no. 2 is shown solid

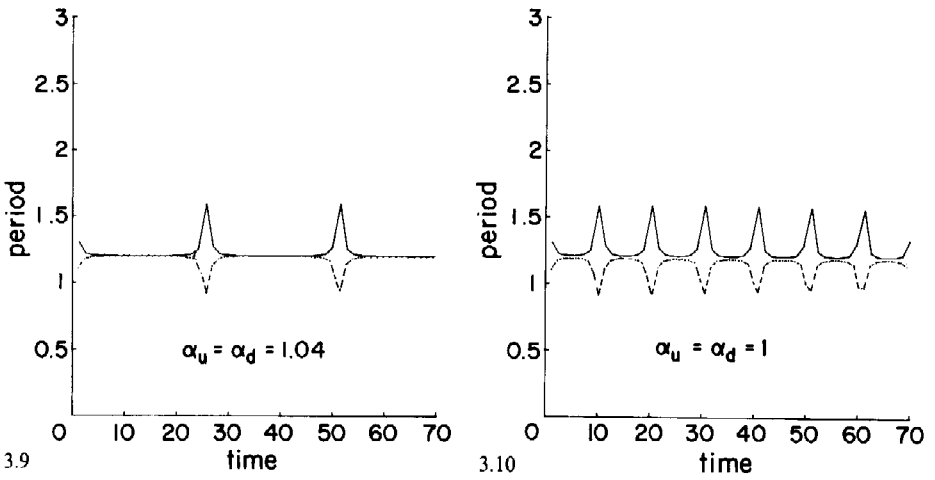

Fig. 3.9. Behavior of two oscillator model: period versus time plot for drifting (but nearly phase locked) case, $\alpha_u = \alpha_d = 1.04$

Fig. 3.10. Behavior of two oscillator model: period versus time plot for drifting case, $\alpha_u = \alpha_d = 1$

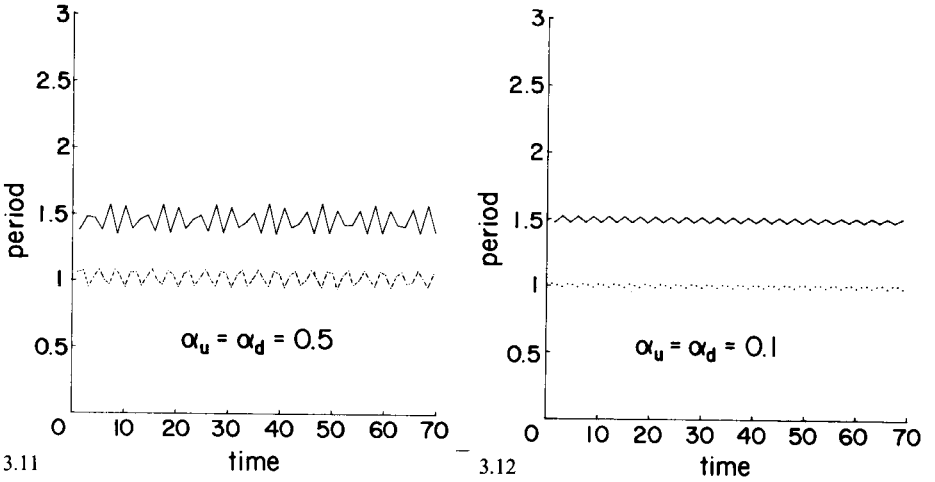

Fig. 3.11. Behavior of two oscillator model: period versus time plot for drifting case, $\alpha_u = \alpha_d = 0.5$

Fig. 3.12. Behavior of two oscillator model: period versus time plot for drifting case, $\alpha_u = \alpha_d = 0.1$

the nature of the loss of phase locking due to a decrease in coupling (e.g. due to a lesion). For $\alpha_u = \alpha_d = 0.5$ the oscillators are largely uncoupled, their periods varying somewhat about their respective uncoupled values (Fig. 3.11). Decreasing the coupling to $\alpha_u = \alpha_d = 0.1$ further extends this trend (Fig. 3.12).

Similar results hold for zero and negative values of the coupling coefficients α_u, α_d. See Fig. 3.13 for which $\alpha_u = 0$, $\alpha_d = 1.5$. This represents the case of one-way

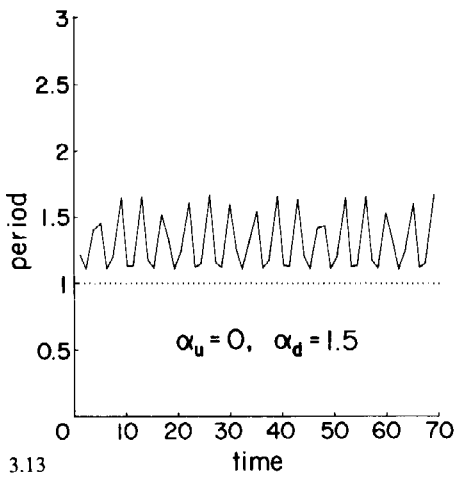

3.13

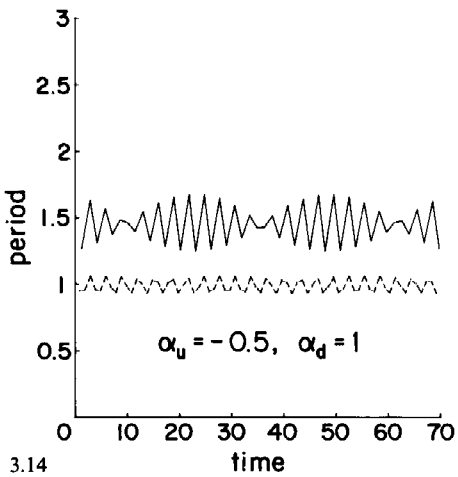

3.14

Fig. 3.13. Behavior of two oscillator model: period versus time plot for case of one-way coupling, $\alpha_u = 0$, $\alpha_d = 1.5$

Fig. 3.14. Behavior of two oscillator model: period versus time plot for drifting case with unequal coupling, $\alpha_u = -0.5$, $\alpha_d = 1$

coupling in which the driving oscillator (here no. 1) fails to entrain the other. Figure 3.14 displays the case $\alpha_u = -0.5$, $\alpha_d = 1$ in which oscillator no. 1 has an excitatory effect on oscillator no. 2, while oscillator no. 2 has an inhibitory effect on oscillator no. 1.

4. Discussion

Comparison of Experimental Lesion Results with Transient Model Behavior

In Fig. 1.3 we see that following a lesion of the lateral tracts, the caudal segments exhibited a great degree of instability while the rostral segments were relatively unaffected. Comparison of Fig. 1.3 with Figs. 3.7–3.14 suggests similarities between the lesioned cord in this example and the simplified two oscillator model described above with $\alpha_u = 0$, $\alpha_d = 1.5$ (i.e., one way coupling, Figs. 3.13, 3.14). This in turn suggests that coordinating fibers which primarily descended head to tail remained in the uncut medial tracts. In the second experiment illustrated which spared the lateral tracts (Fig. 1.4) rostral and caudal segments exhibited comparable disturbances. Comparison with the two oscillator model suggests that this type of lesion might correspond to a decrease in both α_u and α_d, from values sufficiently large to cause phase locking in the intact cord, Eq. (3.8), to smaller values associated with transient behavior (cf. Fig. 3.11, $\alpha_u = \alpha_d = 0.5$). Thus we would expect to find both descending and ascending fibers in the lateral tracts.

The experimental and model systems clearly differ in several respects. For example, in both experiments illustrated the periods of the cord varied more chaotically in the experiment than in the model; furthermore, the simplified two oscillator model does not exhibit the 2 : 1 and 3 : 1 subharmonic locking which has

been observed. In the two oscillator model discussed above, nearest neighbor coupling has been assumed and, as shown in section 3, the forward going traveling wave of normal fictive swimming results from that model if and only if the rostral oscillators run faster than the caudal oscillators. Since some cord fragments exhibit the opposite tendency, this model cannot encompass all our data. However, the 3 oscillator chain with ascending (long-distance) inhibitory coupling can exhibit forward going waves when either rostral or caudal oscillators are fastest. This is, of course, a generalization of the simple nearest-neighbor model and more complex, multi-oscillator generalizations may yield more realistic behavior.

In principle, the properties of the long distance (inhibitory) coupling fibers can be tested experimentally by attempting to locate and cut, or block pharmacologically the relevant fibers. The model predicts a change in phase lag (as β varies in Fig. 3.5, for example), which should be observable. Similarly, it may be possible to construct a more complete coupling matrix α_{ij} (cf. Eq. (2.13)) for a multi-oscillator model by careful experimental measurements involving the stimulation of a given identified fiber and the response of a given segmental oscillator.

Frequency Control

One factor which we have so far neglected in our model is frequency control. As mentioned in the introduction, the speed with which the fish travels through the water is a function of the frequency of the traveling waves which pass down the fish's body. The question arises, how does the system effect a change in the speed of swimming (i.e., a change in the frequency of the traveling waves)? We must reject the notion that the brain emits a variable frequency signal which drives the chain of segmental oscillators. However appealing from the point of view of traditional engineering vibration problems, this is ruled out by the observation that following removal of the lamprey's brain the oscillators burst rhythmically and become entrained, exhibiting essentially normal phase locked behavior. The frequency of the bursting can then be altered by adjusting the concentration of the stimulating drug in the bath (Poon, 1980). Presumably, the drug in the bath is mimicking the action of some substance released from nerve fibers along the length of the cord; whether such a substance acts as a classic neurotransmitter to speed segmental oscillators or as a neuromodulator (cf. Dismukes, 1979) can at present only be speculation.

Such chemical control is consistent with the view that the frequency control is effected locally by altering the frequency ω_i of each of the individual segmental oscillator pairs. In this view, it would be plausible that the decision to change swimming speed could be made in the brain with some of the tracts of the cord transmitting the signal which causes the release of the active compound. Some such control must exist, but the question remains as to the location of the fibers which control frequency, how they function and how they themselves are controlled.

Conclusions

In the models described above, several organizational schemes for the CPG are outlined. All have deficiencies at present but they permit some statements regarding

central pattern generators in general. The first point of interest is that in all our models bidirectional coupling between the oscillators can generate a stable traveling wave. More striking is that in our simplest model, a single set of fibers is sufficient for the coordinating system to maintain proper phase coupling when the fish swims either forwards or backwards; it is necessary simply to retune the end oscillators (see section 3 above). Although the situation in the lamprey is more complex, this elegant mechanism could well apply in simpler 2 oscillator systems. One need not posit any complicated arrangement for reversing the direction of propagation; some control center could easily retune the oscillators when necessary. Whether other systems of multiple coupled oscillators such as that of the leech (Friesen and Stent, 1977) utilize this type of control mechanism is unknown, but could be tested.

It remains unclear how the lamprey cord is structured. First, more data are required to characterize more fully the function and anatomy of the cord. Second, we plan to add elements to the model which would control the frequency and to test other forms of coupling either separately or in combination with the present types. It is not possible to prove that a model is "correct", but with such models as ours it should be possible to test assumptions and formulations which in turn should suggest further experiments and refinements of our concepts.

Acknowledgements. The work of A. Cohen and R. Rand was supported by NIH Grant R01 NS16803, and that of P. Holmes by NSF ENG 78-02891.

References

Berkenblitt, M. B., Deliagina, T. H., Feldman, A. G., Gelfand, I. M., Orlovsky, G. N.: Generation of scratching. I. Activity of spinal interneurons during scratching. J. Neurophysiol. **41**, 1040 – 1057 (1978)

Carpenter, G. A.: Bursting phenomena in excitable membranes. SIAM J. Appl. Math. **36(2)**, 334 – 372 (1979)

Chillingworth, D. R. J.: Differential topology with a view to applications. Pitman, 1976

Cohen, A. H., Buchanan, J. T.: Activity of identified spinal neurons in lamprey during "fictive swimming", Abstract No. 129.2, Soc. Neurosci., 1980

Cohen, A. H., Wallén, P.: The neuronal correlate of locomotion in fish. "Fictive swimming" induced in an in vitro preparation of the lamprey spinal cord. Exp. Brain Res. **41**, 11 – 18 (1980)

Cohen, D. S., Neu, J. C.: Interacting oscillatory chemical reactors. Bifurcation theory and applications in the scientific disciplines. Gurel, O., Rössler, D. E. (eds.). Annals N. Y. Acad. Sci. **316**, 332 – 337 (1979)

Dismukes, R. K.: New concepts of molecular communication among neurons. Beh. Brain Sci. **2**, 409 – 448 (1979)

Ermentrout, G. B.: *n*:*m* phase locking of weakly coupled oscillators. J. Math. Biol. **12**, 327 – 342 (1981)

Friesen, W. O., Stent, G. S.: Generation of a locomotory rhythm by a neural network with recurrent cyclic inhibition. Biol. Cyber. **28**, 27 – 40 (1977)

Getting, P. A., Lennard, P. R., Hume, R. I.: Central pattern generator mediating swimming in *Tritonia*. I. Identification and synaptic interactions. J. Neurophysiol. **44**, 151 – 164 (1980)

Glass, L., Young, R. E.: Structure and dynamics of neural network oscillators. Brain Res. **179**, 207 – 218 (1979)

Grasman, J., Jansen, M. J. W.: Mutually synchronized relaxation oscillators as prototypes of oscillating systems in biology. J. Math. Biol. **7**, 171 – 197 (1979)

Grillner, S.: On the generation of locomotion in the spinal dogfish. Exp. Brain Res. **20**, 459 – 470 (1975)

Grillner, S.: Locomotion in vertebrates: Central mechanisms and reflex interaction. Physiol. Rev. **55**, 247 – 304 (1975)

Grillner, S., Kashin, S.: On the generation and performance of swimming in fish. In: Neural control of locomotion. (Herman, R., Grillner, S., Stein, P., Stuart, D., eds). Vol. 18, pp. 181 – 202. New York: Plenum Press 1976

Grillner, S., Zangger, P.: How detailed is the central pattern generator for locomotion? Brain Res. **88**, 367 – 371 (1975)

Holmes, P. J.: Phase locking and chaos in coupled limit cycle oscillators. Proc. Symp. on Recent Advances in Structural Dynamics, Southampton, England, 1980

Keener, J. P., Hoppensteadt, F. C., Rinzel, J.: Integrate-and-fire models of nerve membrane response to oscillatory input. SIAM J. Appl. Math. (in press)

Kristan, W. B.: Neural control of movement. Group report. In: Function and formation of neural systems (Stent, G. S., ed.), pp. 329 – 354. Berlin: Dahlem Konferenz, 1977

Linkens, D. A.: Analytical solution of large numbers of mutually coupled nearly sinusoidal oscillators. IEEE Trans. Circuits and Systems, CAS-**21(2)**, 294 – 300 (1974)

Linkens, D. A.: Stability of entrainment conditions for a particular form of mutually coupled van der Pol oscillators. IEEE Trans. Circuits and Systems, CAS-**23(2)**, 113 – 121 (1976)

Neu, J. C.: Coupled chemical oscillators. SIAM J. Appl. Math. **37(2)**, 307 – 315 (1979)

Neu, J. C.: The method of near-identity transformations and its applications. SIAM J. Appl. Math. **38(2)**, 189 – 208 (1980)

Neu, J. C.: Large populations of coupled chemical oscillators. SIAM J. Appl. Math. **38(2)**, 305 – 316 (1980)

Pavlidis, T.: Biological oscillators: Their mathematical analysis. Academic Press, 1973

Pavlidis, T., Pinsker, H. M.: Oscillator theory and neurophysiology. Fed. Proc. **36**, 2033 – 2035 (1977)

Pinsker, H. M., Bell, J.: Phase plane description of endogenous neuronal oscillators in *Aplysia*. Biol. Cyber. (in press)

Poon, M. L. T.: Induction of swimming in lamprey by L-DOPA and amino acids. J. Comp. Physiol. **136**, 337 – 344 (1980)

Poon, M., Friesen, W. D., Stent, G. S.: Neural control of swimming in the medicinal leech. V. Connections between the oscillatory interneurons and the motor neurons. J. Exp. Biol. **75**, 45 – 63 (1978)

Rand, R. H., Holmes, P. J.: Bifurcation of periodic motions in two weakly coupled van der Pol oscillators. Int. J. Nonlinear Mechanics **15**, 387 – 399 (1980)

Rovainen, C. M.: Neurobiology of lampreys. Physiol. Rev. **59**, 1007 – 1077 (1979)

Russell, D. F., Wallén, P.: On the pattern generator for fictive swimming in the lamprey, *Icthyomyzon unicuspis*. Acta Physiol. Scand. (abst.) (1979)

Selverston, A. I.: Are central pattern generators understandable? Beh. Brain Sci. **3**, 535 – 571 (1980)

Selverston, A. I., Russell, D. F., Miller, J. P., King, D. G.: The stomatogastric nervous system; structure and function of a small neural network. Prog. Neurobiol. **6**, 1 – 75 (1976)

Stein, P. S. G.: Mechanisms of interlimb phase control. In: Neural control of locomotion (Herman, R., Grillner, S., Stein, P., Stuart, D., eds.). Vol. 18, pp. 465 – 487. New York: Plenum Press 1976

Tang, D., Selzer, M. E.: Projections of lamprey spinal neurons determined by the retrograde axonal transport of horseradish peroxidase. J. Comp. Neurol. **188**, 629 – 646 (1979)

Vidal, C., Viala, D., Buser, P.: Central locomotor programming in the rabbit. Brain Res. **168**, 57 – 73 (1979)

Wilson, D. M.: The central nervous control of flight in a locust. J. Exp. Biol. **38**, 471 – 479 (1961)

Received April 7/Revised August 10, 1981